

Synthesis of a Novel Fuel Additive Solketal Levulinate by using MOF ZIF-8 and SSA Loaded PVA Functional Catalytic Membrane

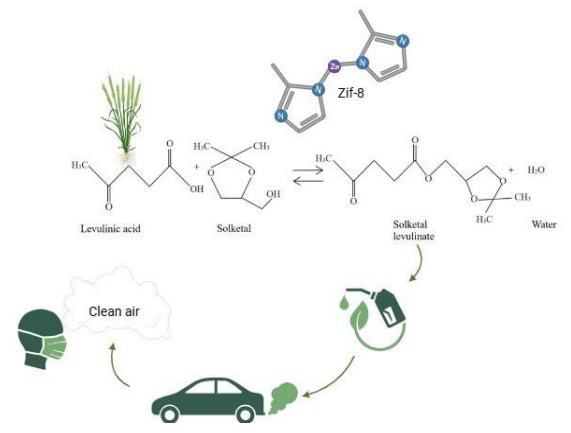
Nazli Yuzer¹ and Nilufer Hilmioglu^{1*}

¹Chemical Engineering Department of Kocaeli University, İzmit, Kocaeli, Turkey Received: 03/06/2025, Accepted: 16/10/2025, Available online: 20/10/2025

*to whom all correspondence should be addressed: e-mail: niluferh@kocaeli.edu.tr

https://doi.org/10.30955/gnj.07727

Graphical abstract



Abstract

Solketal levulinate (SoLE), a potential fuel additive that can improve the physicochemical properties of the fuel, was produced by the developed catalytic membrane from solketal and levulinic acid. The catalytic membrane was prepared in film form as a metal-organic framework of ZIF-8 supported on a sulfosuccinic acid-loaded hydrophilic polyvinyl alcohol polymer. Removing by-product water from the reaction medium with the sorption of the highly hydrophilic membrane contributed to the conversion. PVA/SSA and PVA/SSA/ZIF-8 membranes were analyzed by FTIR and TGA. ZIF-8 was photographed and analyzed by SEM and XRD, respectively. Higher water affinity of the functional catalytic membranes was calculated by swelling degree and interaction parameter calculations. SoLE synthesis was conducted in the batch reactor under mild conditions. The parameters such as catalyst amount, temperature, solketal/levulinic acid initial molar ratio (M), and reaction time, were investigated. The PVA/SSA catalytic membrane showed a maximum reaction conversion of 97.65% with 105°C, 9 mmol SSA, and an M:6/1 ratio for 6h. For the PVA/SSA/ZIF-8 catalytic membrane, maximum reaction conversion of 96.81% was obtained at 105°C, with an M:6/1 ratio and 9 mmol SSA for 4 hours. ZIF-8 reduced the reaction time and contributed to the system in terms of efficient energy use.

Keywords: Esterification, levulinic acid, heterogeneous catalyst, Bio-additive

1. Introduction

The need for energy reserves in the world is rapidly increasing in direct proportion to the growing human population. Fossil fuel reserves are in danger of exhaustion, which has increased the search for alternative fuels to satisfy energy needs. Interest in the development of green(clean)-content fuels has increased at the outset of a wide range of studies in this direction, as they are both environmentally friendly and renewable resources (Singh et al. 2023). The major problem related to combustion events of bio-based and green-content fuels, which are frequently investigated in the literature, is a key focus of research. Whether the fuels/fuels additive are fossil or green and sustainable fuels, the production of new generation fuel additives to improve the combustion properties of these fuels is an important step towards solving this problem. Toxic emissions from the combustion of fuels are reduced by optimizing engines and equipment, using catalytic converters, NOx reducers, and particulate filters for engine-based uses, as well as modifications to the chemical composition of the fuels (Çakmak and Özcan 2018). In addition to conventional methods (isomerization, catalytic cracking, reforming-dehydrocyclization), oxygenrich fuel additives and oxygenates can be added to improve the octane number of gasoline and the cetane number of diesel. However, traditional methods are costly and difficult. The octane number of gasoline or the cetane number of diesel are improved by adding oxygenates such as oxygenated alcohols and ethers after the refining of crude oil (Demirbas et al. 2015). Bio-ethanol, which is the leading bio-based fuel additive, can be obtained chemically or through fermentation. However, in both situations, long-term production processes cause both carbon emissions and system costs to increase. This makes the production process less environmentally friendly (Mussatto et al. 2010). Commonly encountered levulinatebased oxygenates in the literature include ethyl levulinate, methyl levulinate, and SoLE. However, these levulinatebased fuel additives are mainly produced by the reaction of alcohols or ketals with oxo-carboxylic acid anions (methyl levulinate, ethyl levulinate, etc.) (Jia et al. 2020). In such reactions, alcohols are used as reactants or as by-products, and these alcohols (except ethanol) are highly toxic and

ecologically hazardous (Xu et al. 2020). Solketal levulinate (SoLE) is a potential levulinate-based fuel additive that improves the cold flow properties of the fuel (Mariam et al. 2024; Mariam et al. 2021). As shown in Figure 1, SoLE can be synthesized from solketal and levulinic acid (Sutinno 2016). This reaction, levulinic acid esterification, is a very environmentally friendly reaction in terms of both reactants and products. In addition, it produces no harmful waste. There are very few studies in the literature on the synthesis of SoLE from solketal and levulinate esters. In this study, SoLE was synthesized from solketal and levulinic acid for the first time. Levulinic acid (LA), a 5-carbon ketoacid, is one of the twelve platform chemicals defined by the US Department of Energy that can be produced from biomass; an environmentally friendly alternative to petroleumbased chemical production (Jeanmard et al. 2025). There are numerous commercial chemicals produced from LA, such as aminolevulinic acid (DALA), diphenolic acid (DPA), methyl tetrahydrofuran, various esters, and resins. Fuel additives can also be synthesized from LA, a highly versatile building block chemical. (Sajid et al. 2021; Ethiraj et al. 2022). Solketal, which is also used as a reactant in its synthesis, is a renewable and green solvent and can be used alone as an environmentally friendly fuel additive (Fernández et al. 2019; Ilgen et al. 2017). Polyvinyl alcohol (PVA) а highly hydrophilic, biocompatible, is environmentally friendly, functional synthetic polymer that can form good films. Due to its high hydrophilicity in reactions where water is a by-product, PVA can provide sorption support to the reaction to remove the by-product and direct the reaction equilibrium to the product side (Song et al. 2023; Unlu and Hilmioglu 2019). Sulfosuccinic acid (SSA), which can be bio-based and sustainable, is a highly effective catalyst when added to the catalytic membrane, especially in esterification reactions due to its acidic nature (Portillo Perez et al. 2023). Zeolitic imidazolium framework-8 (ZIF-8), used as a support material in the catalytic membrane, is a type of metalorganic framework (MOF). MOFs are porous materials comprised of organic ligands and metal ions. They can be used as catalyst supports with their high specific surface area, microporosity, and finely tunable chemical and physical properties (Doan et al. 2025; Wi'sniewska et al. 2023; Laeim et al. 2025). Catalytic membranes, which are environmentally friendly functional catalysts, often composed of polymeric matrices and catalysts, are bifunctional materials that direct the reaction equilibrium towards product formation by removing the by-product of the reaction through sorption support (Hasirci et al. 2023). Studies on the synthesis of SoLE are very limited in the literature, and the synthesis was carried out by a transesterification reaction using a base catalyst. Mariam et al. 2021 synthesized SoLE from solketal and methyl levulinate as a potential fuel additive for palm biodiesel. They achieved a maximum yield of 74.83% at 140°C and 1.5% catalyst loading with Methyl levulinate/Solketal at a molar ratio of 1:4 for 6 hours. Liu et al. 2024, produced methyl levulinate glycerol ketal from methyl levulinate and glycerol. The influence of different parameters on methyl levulinate glycerol ketal yield and glycerol conversion were

investigated. The optimum conditions were determined as temperature T = 140 °C, catalyst loading of 0.50 g HZSM-5, and ML/GLY mol ratio of 4:1. Under these conditions, glycerol conversion was 97%, and methyl levulinate glycerol ketal yield was 94.7%. SoLE can be manufactured by acid-catalyzed esterification of solketal and levulinic acid (Mariam et al. 2021; Sutinno 2016). Esterification reactions are processes in which water is produced as a by-product (Moradi et al. 2021). Water removal from the reaction medium shifts the equilibrium towards the products and increases the reaction conversion (Hilmioglu 2022). For the first time in the literature, SoLE was synthesized from solketal and levulinic acid in a batch reactor using a catalytic membrane. Blending catalysts used in the reaction with suitable polymer solutions to convert them from homogeneous to heterogeneous form is an excellent way to produce catalytic membranes. In this study, ZIF-8, used as a support material with an MOF cage structure was synthesized, functionalized with sulfosuccinic acid (SSA) with high Brönsted acid sites, and blended with PVA polymer to prepare catalytic membranes. In the context of Sole production, green catalytic membranes have not been used in the literature before. Reactions with catalytic membranes are hybrid systems in which both the reaction with the catalyst and the separation of the desired product or by-product, according to the properties of the membrane material used (hydrophilic or hydrophobic), from the environment can be performed simultaneously in a single unit. For this reason, the contribution of this research article, to the literature, is promising for future studies.

This study established an experimental batch reactor system by placing catalytic membrane pieces inside. Ease of operation and re-use of the catalyst is enabled by the batch reactor, in which the reaction and sorption of the byproduct occur simultaneously. This shifts the reaction balance towards the product and increases conversion without using extra reactants. The reaction was shown in **Figure 1**

Figure 1. Solketal levulinate synthesis from Levulinic acid and Solketal (Sutinno 2016)

2. Materials and Methods

2.1. Materials

PVA in solid form (MW~125,000), SA (70% in water), and 2-methylimidazole were obtained from Sigma-Aldrich; zinc nitrate hexahydrate (Zn (NO₃)₂-6H₂O) was obtained from Acros Organics, while LA (for synthesis) was obtained from Merck Chemicals. Solketal was purchased from BLD Farm.

2.2. ZIF-8 synthesis

ZIF-8 was synthesized by the rapid addition of an aqueous solution of Zn (NO₃)₂·6H₂O to an aqueous solution of 2-methylimidazole. Firstly, 1.17 g of zinc nitrate was dissolved

in 8 g of distilled water. Then, 22.70 g of 2-methylimidazole was dissolved separately in 80 g of distilled water. These two solutions were combined and stirred at room temperature until a turbid solution was formed. It was then centrifuged, and the ZIF-8 precipitate obtained was dried at 80 °C overnight (Pan et al. 2011).

2.3. Preparation of PVA/SSA and PVA/SSA/ZIF-8 Functional Catalytic Membranes

3, 6, and 9 mmol of SSA were added respectively to 6% PVA solutions, each prepared in certain predetermined amounts. The PVA-catalyst mixture was stirred for 1 hour and then poured onto Teflon plates and was left to dry. The dried membranes were then heat treated at 120 °C for 1 hour for crosslinking. For the preparation of ZIF-8 doped PVA/SSA membranes, 0.1 g ZIF-8 was added to PVA solutions. After stirring the PVA-ZIF-8 mixture for 1 hour, either 3, 6, or 9 mmol of SSA were added, and the mixture was further stirred. In the last step, PVA/ZIF-8/SSA mixtures were poured onto Teflon plates and left to dry at room temperature. As before, dried membranes were heat-treated at 120 °C for 1 h for crosslinking.

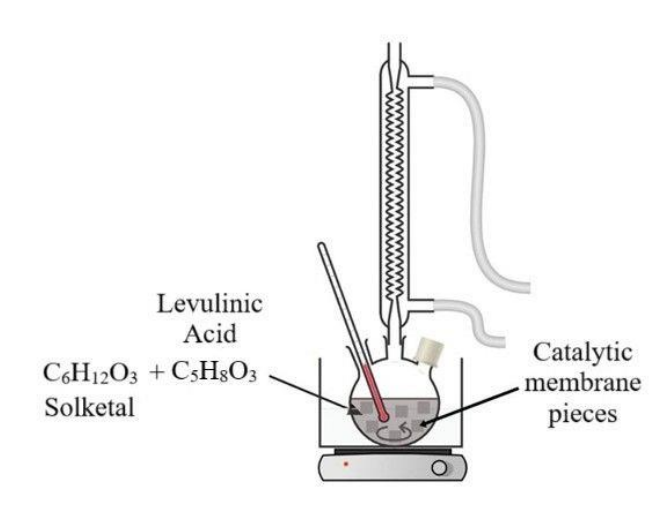


Figure 2. Batch Reactor system

2.4. Batch Reactions

Solketal levulinate reaction was carried out with PVA/SSA and PVA/SSA/ZIF-8 functional catalytic membranes at 105°C. The loading of SSA acid catalyst in the catalytic membranes used in the reaction was 3, 6, 9 mmol and the initial molar ratios for Solketal/Levulinic Acid were chosen as 4/1, 5/1, 6/1. The batch reactor is shown in **Figure 2**.

2.5. Analysis of Reaction Products

The catalytic performance of PVA/SSA and PVA/SSA/ZIF-8 functional catalytic membranes was analyzed by the titration method, with LA conversion calculated by Equation 1 (Unlu and Hilmioglu 2016)

$$X = \frac{N_{Ao} - N_A}{N_{Ao}} \tag{1}$$

 N_{Ao} is the number of moles of levulinic acid in solution at the beginning, and N_A is the number of moles of levulinic acid at any given time.

3. Results and Discussions

3.1. Fourier-transform infrared spectroscopy (FTIR) characterization of PVA/SSA and PVA/SSA/ZIF-8 catalytic Membranes

Figure 3 shows the FTIR spectra of pure PVA, PVA/SSA, and PVA/SSA/ZIF-8 functional catalytic membranes. The characteristic peak observed at 3260 cm⁻¹ wavenumber in pure PVA belongs to the O-H stretching band, while the characteristic absorbance peak at 1096 cm⁻¹ is due to the C-O stretching (Khatuaa et al. 2015; Norouzi et al. 2021). When PVA/SSA functional catalytic membranes were examined, the O-H stretching band observed at 3260 cm⁻¹ shifted to 3365 cm⁻¹ upon addition of SSA to the structure. (Rynkowska et al. 2019). The peak observed at a wavelength of 1035 cm⁻¹ is associated with the stretching vibration of the S-O bond, indicating the presence of SSA. 1725 cm⁻¹ represents the C=O bond of SSA (Ngo et al. 2022). For PVA/SSA/ZIF-8, when ZIF-8 was added to the polymer matrix, it was observed that the peak intensity of the hydroxyl groups in the structure decreased. This can be explained by the high hydrophobicity of ZIF-8 (Yang et al. 2021).

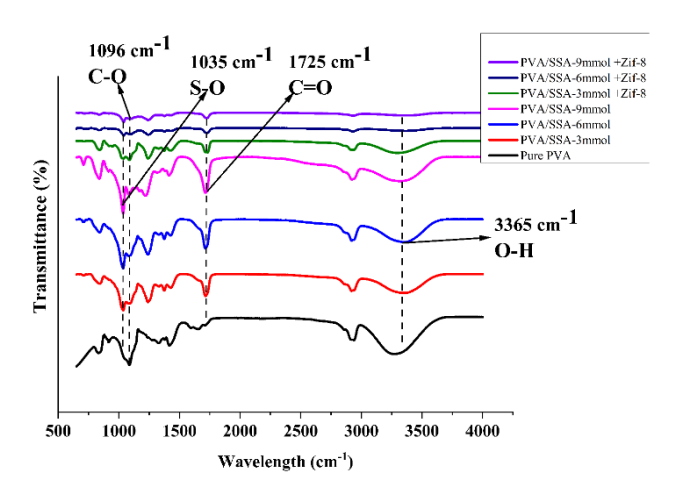


Figure 3. FT-IR of PVA/SSA and PVA/SSA/ZIF-8 catalytic membranes

3.2. Thermogravimetric analysis (TGA) of PVA/SSA and PVA/SSA/ZIF-8 catalytic membranes

Three degradation regions were observed in the TGA curves of PVA/SSA and PVA/SSA/ZIF-8 catalytic membranes, shown in Figure 4. While the first degradation in the 100°C-210°C temperature range is due to the elimination of water in the structure, the degradation in the second region from 210°C to 300°C is related to the detachment of sulfonic groups from the ester bonds between SSA and PVA. The polymer chain decomposed in the last region (between 420 °C and 500 °C) (Gomaa et al. 2017; Maarouf et al. 2020). According to the TGA curves for PVA/SSA catalytic membranes, SSA added to PVA increased the thermal stability compared to pure PVA. In addition, the amount of residue at the end of the analysis increased directly with the amount of SSA (Rynkowska et al. 2019). No significant effect of ZIF-8 on thermal stability was observed.

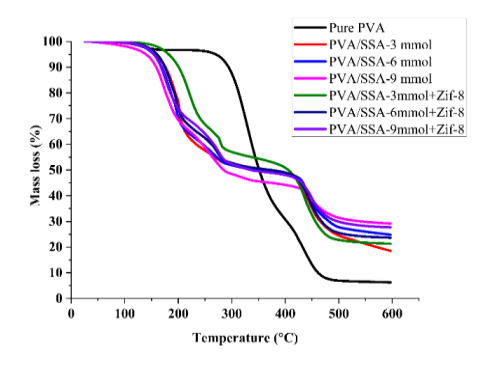


Figure 4. TGA of PVA/SSA and PVA/SSA/ZIF-8 catalytic membranes.

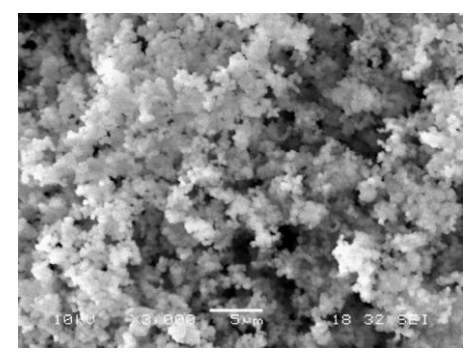


Figure 5. SEM image of ZIF-8 Crystals.

Table 1. N₂ Adsorption/Desorption Data for the MOF of ZIF-8

Intensity (cps)	5	10	15	20	لېل ـــــــــــــــــــــــــــــــــــ	بيمال ــــــــــــــــــــــــــــــــــــ	35	40	45	50
,	, ,	10	15		25 2-thet:		35	40	45	50
						-				

Figure 6. XRD of ZIF-8.

3.3. Scanning Electron Microscopy (SEM) and X-Ray Diffraction Analysis (XRD) Analyses of Synthesized ZIF-8

SEM image of the produced ZIF-8 is shown in **Figure 5**. The SEM image of ZIF-8 is similar to the images in other studies in the literature (Attwa *et al.* 2024). The morphology of ZIF-8 contains spherical ZIF-8 crystals (Thi Thanh *et al.*). XRD peaks of produced ZIF-8 are shown in **Figure 6**. The high-intensity diffraction peak at $2\theta = 7.36$ is an important characteristic peak of ZIF-8, indicating its high crystallinity (Qiu *et al.* 2022; Thi Thanh *et al.* 2017; Nordin *et al.* 2017).

3.4. BET Analysis of ZIF-8

Table 1 shows the results of the BET analysis of ZIF-8.

Adsorbent (MOF ZIF-8)				
S _{BET} (m ² /g)	1831.70			
Total Pore Volume (V _p (cm ³ /g))	0.67			
Average Pore Size (Å)	14.55			
BJH Adsorption Pore Diameter (Å)	49.54			
BJH Desorption Pore Diameter ()	38.93			
HK Method Pore Diameter (Å)	4.32			
SF Method Pore Diameter (Å)	6.18			

Figure 7 shows that ZIF-8 exhibits Type I isotherms according to the IUPAC classification. A significant increase in the amount adsorbed was observed at low P/P₀ values (0.015 P/P0 0.1). This result is typical for solid materials with microporous structures such as ZIF-8. According to the BET analysis, the specific surface area is 1831 m²/g, the total pore volume at P/P₀ = 0.99 is 0.66 cm³/g, and the pore size has a peak at 6.18 Å. Considering the range of 6.18 Å, where the peak is strongly observed, the pore size distribution shows that the material has a largely microporous structure. (Kruk and Jaroniec 2001; Pan *et al.* 2011; Missaoui *et al.* 2022; Zhang *et al.* 2022)

3.5. Swelling Tests of PVA/SSA and PVA/SSA/ZIF-8 Catalytic Membranes

Swelling tests are performed to determine the affinity of a material for its solvent or reactants and products, if the material is to be used in a reaction medium. In this study, the synthesis of SoLE is an esterification reaction that releases water as a by-product. The presence of water in the reaction environment causes the reaction equilibrium to be directed to the side of the reactants, reducing the reaction yield. It is possible to shift the reaction towards product formation (Le Chatelier's Principle) by continuously removing water from the reaction medium

(Liu and Ma 2024; Zhu Jie *et al.* 2024). Therefore, the functional catalytic membrane must be hydrophilic. The water swelling results for the pure PVA, PVA/SSA, and PVA/SSA/ZIF-8 functional catalytic membranes used in the reaction are given in Tables 2 and 3. Water swelling rates were calculated with Equation (2).

$$R_{e} = \left\lceil \left(R_{L} / a_{eq}\right) - \left(RH f_{ad} R_{ad}\right)\right\rceil / \left\lceil \left(\left(1 - RH\right) / a_{kin}\right) + RH \left(1 - f_{ad}\right)\right\rceil \tag{6}$$

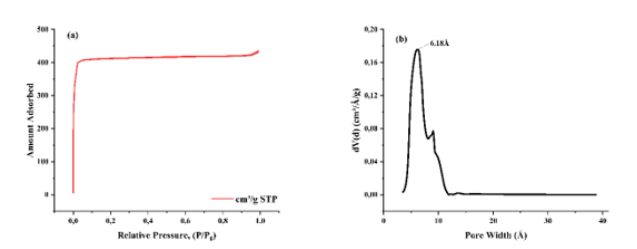


Figure 7. (a) N₂ Adsorption/Desorption Isotherms Data for ZIF-8; (b) Pore Width(Å) for ZIF-8.

Swelling(%)=
$$\frac{W_{\text{wet}} - W_{\text{dry}}}{W_{\text{dry}}} \times 100$$
 (6)

In Equation 2; W_{wet} and W_{dry} signify wet catalytic membrane weight (g) and dry catalytic membrane weight (g), successively.

Table 2. Swelling tests of PVA/SSA catalytic membranes.

Catalytic membrane	Swelling Rate (%)
Pure PVA	755.2
PVA/SSA-3 mmol	401.3
PVA/SSA-6 mmol	499.4
PVA/SSA-9 mmol	553.8

Table 2 shows that when SSA was added to PVA, the swelling rate decreased compared to pure PVA. The heat treatment after the addition of SSA reduced the swelling rate by cross-linking. As the amount of SSA in the catalytic membrane increased, the swelling ratios rose due to the increased number of hydrophilic sulfonic acid groups (Yagizatli *et al.* 2022). In **Table 3**, when ZIF-8 was added to the PVA/SSA catalytic membrane structure, a decrease in the swelling ratio was observed due to the hydrophobic effect of ZIF-8. (Sann *et al.* 2018).

Table 3. Swelling tests PVA/SSA/ZIF-8 catalytic membranes

Catalytic membrane	Swelling Rate (%)
Pure PVA	755.2
PVA/SSA-3 mmol+ZIF-8	381.5
PVA/SSA-6 mmol+ZIF-8	419.7
PVA/SSA-9 mmol+ZIF-8	483.1

3.6. Contact Angle Testing

In this study, esterification reaction was carried out with solketal and levulinic acid as reactants and solketal levulinate was obtained as product. However, the accumulation of water as a by-product in the reaction medium will reduce the product yield/reaction conversion and needs to be removed. Therefore, for the preparation of the catalytic membrane used in the reaction, PVA polymer, which is highly hydrophilic, thermally and chemically stable and environmentally friendly thanks to the hydroxyl groups it contains, was chosen; hydrophilicity or hydrophobicity in a material is explained as the ability of the selected material to bind to water molecules with hydrogen bonds on the part of its surface in contact with water ((Li W. et. al. 2013; Rezaee et. al. 2015; Yadav D. et. al. 2022). Water was used in the contact angle test to understand the hydrophilicity of the prepared membranes. When the liquid makes an angle of less than 90° with the contact surface, it indicates hydrophilicity, while an angle of more than 90° indicates hydrophobicity (Milne A. J. B. and Amirfazli A. 2009).

Zeolitic imidazolate frameworks (ZIFs), a subfamily of MOFs, are materials with the ability to tune their pore size and high chemical functionality while ZIF-8s are a new type with zeolite topology and have excellent chemical stability and high structural diversity found in all zeolite varieties. Its high chemical properties and thermally stable behavior indicate that it can be easily recycled from its environment in the process of use. ZIF-8 has a large surface area, strong and high degree of hydrophobicity (145°) and superoleophilic properties (San E. E. et al. 2018; Zhang K. et al. 2013).

Hydrophobicity/Hydrophilicity property is shown in **Figure 8** with contact angle values.

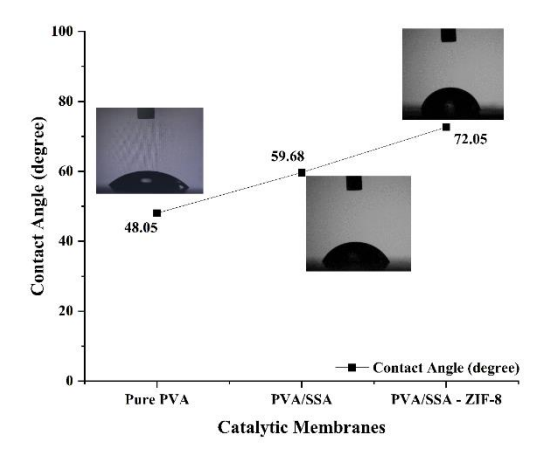


Figure 8. Contact Angles Degree of Pure PVA, PVA/SSA and PVA/SSA – ZIF-8

The addition of ZIF-8, which has high hydrophobicity, to the prepared PVA-based catalytic membrane brought the PVA polymer, which has high hydrophilicity, closer to its hydrophobicity. It is predicted that this gain in the catalytic membrane will provide energy efficiency by reducing the reaction time.

3.7. Interaction Parameters of PVA/SSA Catalytic membranes

The interaction between the by-product water and the polymer matrix of the catalytic membrane is well explained by the Flory-Huggins interaction parameter calculations. The Flory-Huggins interaction parameter helps to explain the interaction between a solvent and a polymer, based the amount of liquid sorbed by the polymer. As the interaction parameter approaches zero, the affinity of the polymer for the solvent increases (Nistane *et al.* 2022). The interaction parameters for each SSA amount were calculated by Equations 3, 4, and 5.

$$\Phi_{s} = \frac{\frac{Q}{\rho_{s}}}{\frac{Q}{\rho_{s}} + \frac{1}{\rho_{p}}}$$

$$(3)$$

$$\Phi_{\rm p} = 1 - \Phi_{\rm s} \tag{4}$$

$$X_{ip} = -\frac{\ln(1 - \Phi_p) + \Phi_p}{\Phi_p^2}$$
 (5)

Here, Xip is the interaction parameter and dimensionless; Q (g/g) is the weight of water sorbed by one gram of polymeric membrane; ps (g/cm³) and pp (g/cm³) are densities of water and polymer, respectively. Φ_p and Φ_s are volume fractions of polymer and water, respectively. (Huang 1991). The interaction parameters calculated for PVA/SSA catalytic membranes are shown in Table 4. A decrease in the values of the interaction parameters was observed as a result of increasing hydrophilicity with increasing number of hydrophilic sulfonic acid groups (Hasirci *et al.* 2023; Ohtake *et al.* 2022).

Table 4. Interaction parameters of PVA/SSA catalytic membranes

Catalytic membrane	Interaction parameter
PVA/SSA-3 mmol	0.521
PVA/SSA-6 mmol	0.486
PVA/SSA-9 mmol	0.439

3.8. Acidity of PVA/SSA and PVA/SSA - ZIF-8 Catalytic Membranes

The acidic or basic properties of catalysts can be explained by the amount of H⁺ / OH⁻ ions in their chemical structure. Although there are different methods in the literature, the most widely used method for determining the amount of acid/base is the ion displacement reaction.

Ion displacement reaction is determined by classical acidbase titration to determine the degree of acidity of a material depending on the acid groups it has. This is done as follows; a certain amount of the material whose acidity is to be determined is taken and kept in 1M NaCl solution for 48 hours. The H+ ions, which are replaced by Na+ ions in the salt solution, are titrated with 0.05 M NaOH together with phenolphthalein, which is prepared before titration and acts as an indicator (Atkar A. et al.,2024). Ion exchange capacity is calculated by Equation 6:

$$IDR \left(\text{mmol H}^{+} \text{ g}^{-1} \right) = \frac{\text{Consumption NaOH (ml)} \times \text{NaOH Molarite}}{\text{Sample Weight}}$$
 (6)

Calculated ion displacements are given in Table 5.

Table 5. Acidity of PVA/SSA and PVA/SSA - ZIF-8 Catalytic Membranes

ACIDITY (mmol H+ g ⁻¹)				
PVA - (w/w) 3mmol SSA	15.23			
PVA - (w/w) 6mmol SSA	>16			
PVA - (w/w) 9mmol SSA	>18			
PVA - (w/w) 3mmol SSA/ZIF-8	15.24			
PVA - (w/w) 6mmol SSA/ZIF-8	>16			
PVA - (w/w) 9mmol SSA/ZIF-8	>18			

Acidity values were also given in Figure 9.

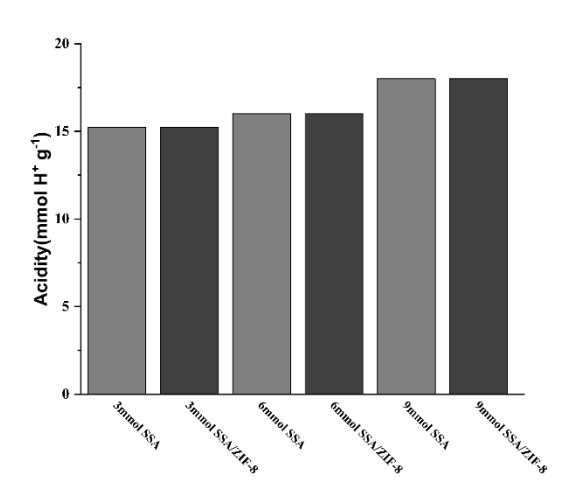


Figure 9. Acidity of PVA/SSA and PVA/SSA - ZIF-8 Catalytic Membranes

3.9. Batch Reactions with PVA/SSA and PVA/SSA/ZIF-8 Catalytic Membranes

Batch reactions with PVA/SSA and PVA/SSA/ZIF-8 catalytic membranes were performed at 105 °C and 3, 6, and 9 mmol SSA loadings, with Solketal/LA: 4/1, 5/1, 6/1 molar ratios. The effect of reaction time, SSA loading, and Solketal/LA ratio on reaction conversion was examined in batch reactions.

3.9.1. Influence of the reaction time on LA conversion

The influence of reaction time on the reaction conversion in the SoLE synthesis with PVA/SSA catalytic membranes at 9 mmol catalyst loading, with Solketal/LA: 6/1, and a reaction temperature of 105°C is given in **Figure 10**. In the reaction carried out over the course of 8 hours, the conversion increased from 9.39% in the 1st hour to 97.65% in the 6th hour, where it reached a maximum. After 6 hours, small decreases in reaction conversion were observed. Since the SoLE synthesis is a reversible reaction, after the 6th hour, the reaction may begin to favor the reactants' side due to the increasing amount of water as a by-product. Therefore, the optimum reaction time was determined to be 6 hours. (Chansorn *et al.* 2022; Zhang *et al.* 2021; Zhu Jishen *et al.* 2024).

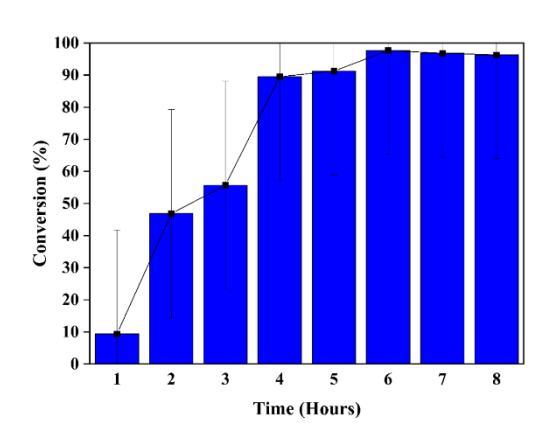


Figure 10. Influence of the reaction time on conversion with PVA/SSA catalytic membranes

To determine the optimized reaction time, SoLE synthesis was carried out with ZIF-8 doped PVA/SSA catalytic membranes at 9 mmol SSA loading, M:6/1 ratio, and 105 °C. As shown in **Figure 11**, the reaction conversion increased from 38.01% at 1 hour to 96.81% at 4 hours. After 4 hours, no significant change in reaction conversion was observed. After 4 hours, the reaction reached an equilibrium state, and there was no significant change in conversion. The hydrophobicity of ZIF-8 prevented the occurrence of the reverse reaction. (Cao *et al.* 2021; Li *et al.* 2023). The optimum reaction time was determined to be 4 hours. The addition of ZIF-8 reduced the reaction time.

Hydrophobic catalysts show high resistance to water. Since esterification reactions are reversible and limited by thermodynamic equilibrium, the hydrophobicity of the catalysts to be used allows the reacting organic molecules to adhere to the catalyst surface, while the desorption of by-product water molecules in esterification reactions and the selection of reactants in the reaction medium accelerate the reaction in the direction of the entrants and accelerate the ester formation (Liu, J. et. al. 2022). For this reason, they are often preferred for their ability to provide

favorable conditions for reactants in esterification reactions. (Ristiana D. D. et. al. 2022; Suryandari A. S. et. al. 2023)

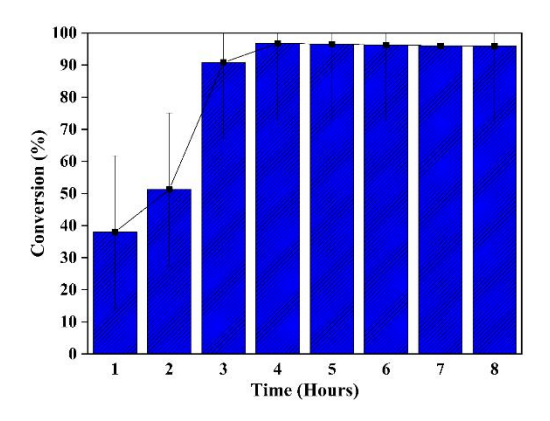


Figure 11. Influence of the reaction time on conversion with PVA/SSA/ZIF-8 catalytic membranes

3.9.2. Influence of SSA loading on LA Conversion

The effect of SSA loading in the PVA/SSA catalytic membrane on LA conversion at 105°C and a 6/1 Solketal/LA ratio for 6 hours is presented in **Figure 12**. The reaction conversion increased from 61.39% at 3 mmol SSA loading to 97.65% at 9 mmol SSA loading. Since the number of catalytically active sites in the membrane increased with increasing catalyst loading, an enhancement in reaction conversion was observed (Zhang *et al.* 2024; Goda *et al.* 2022). However, a minimal difference was observed in terms of reaction conversion at 6 mmol and 9 mmol SSA loading.

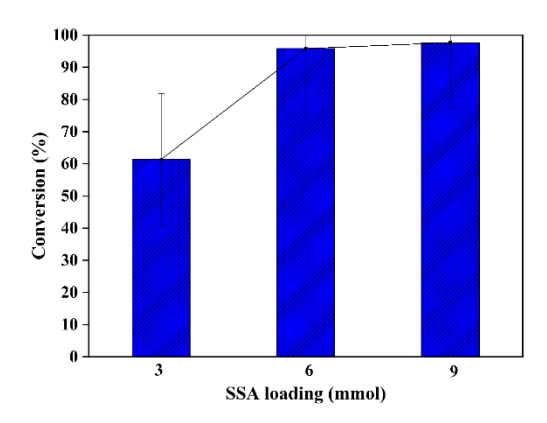


Figure 12. Influence of SSA loading on conversion with PVA/SSA catalytic membranes

At 105 °C and with a ratio of M to 6/1, reactions were performed for 4 hours to observe the effect of the amount of catalyst on the reaction conversion in ZIF-8 doped PVA/SSA membrane. **Figure 13** shows that while 8.75% conversion was obtained at 3 mmol SSA catalyst loading, dramatic increases to conversion rates of 95.06% and 96.81% were obtained when the amount of catalyst was raised to 6 mmol and 9 mmol, respectively. No significant increase in reaction conversion was observed when SSA loading was raised from 6 mmol to 9 mmol (Soltani *et al.* 2021; Al-Saadi *et al.* 2020).

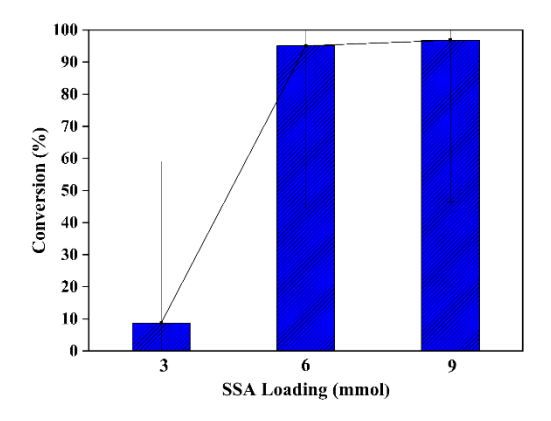


Figure 13. Influence of SSA loading on conversion with PVA/SSA/ZIF-8 catalytic membranes

3.9.3. Influence of Solketal/LA initial molar ratio

To observe the effect of Solketal/LA molar ratio on the conversion with PVA/SSA catalytic membranes, the reactions were carried out at 105°C at a catalyst loading of 9 mmol for 6 hours, as shown in Fig. 14. At the molar ratios examined, very high conversions were obtained with very small differences in yields. While 95.26% conversion was obtained at M 4 to 1 ratio, conversion reached 97.65% at M 6 to 1 ratio. In the synthesis of SoLE (a reversible esterification reaction), feeding excess solketal, into the reaction medium can increase reaction conversion by shifting the balance towards product formation (Guo et al. 2021). However, the concentrations of the reactants and the conversion of the reaction may decrease due to the increasing amount of water, leading to a back reaction. (Cao et al. 2021). Thus, for the given molar ratios, increasing the Solketal/LA molar ratio did not cause a significant increase in the reaction conversion. The optimum molar ratio was determined as 4:1.

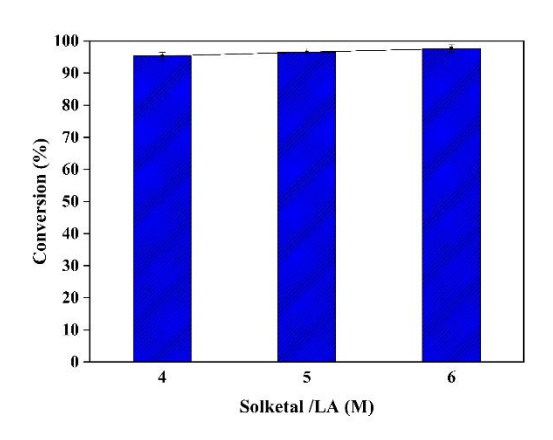


Figure 14. Influence of Solketal/LA molar ratio on conversion with PVA/SSA catalytic membranes

The effect of Solketal/LA molar ratios of 4/1, 5/1, and 6/1 on reaction conversion with PVA/SSA/ZIF-8 catalytic membranes is shown in **Fig. 15**. The conditions of observation are 9 mmol catalyst loading, a 105 °C reaction temperature, and a 4 h reaction time. The reaction conversion was 93.97% at M:4/1, and reached 96.81% at M:6/1. The conversion data of the three different ratios were obtained very close to each other, as shown in **Fig. 12**.

At the given molar ratios, the reaction conversion has reached the limit point (Mao *et al.* 2020). It was observed that the change in the determined molar ratios did not significantly affect reaction conversion.

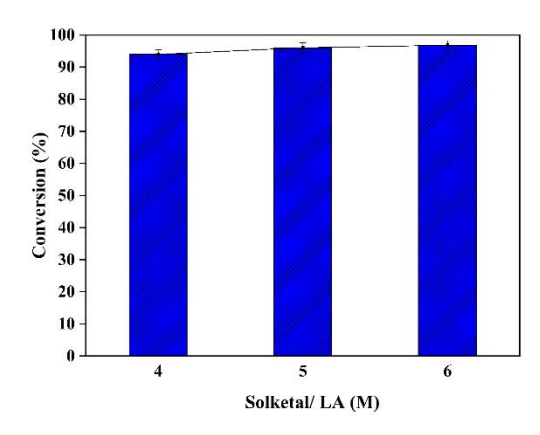


Figure 15. Influence of Solketal/LA molar ratio on conversion with PVA/SSA/ZIF-8 catalytic membranes

4. Conclusions

In this study, a new generation of environmentally friendly fuel additive, solketal levulinate, was synthesized from the esterification of solketal and levulinic acid using functional PVA/SSA and PVA/SSA/ZIF-8 catalytic membranes in a batch reactor under mild conditions for the first time in the literature. Functional catalytic membranes were produced from a PVA matrix, SSA as a catalyst, and ZIF-8, a type of MOF, as a support material. The peak (S-O bond) at 1035 cm⁻¹ in the FTIR analysis of the produced catalytic PVA/SSA membranes confirms the SSA loading. In addition, the presence of ZIF-8 in the PVA/SSA/ZIF-8 catalytic membrane structure increased the hydrophobicity of the structure. In TGA analysis, the integration of SSA to the PVA matrix increased the thermal stability. In swelling tests in water, SSA increased the hydrophilicity of the structure by increasing the extent of swelling. The catalytic membrane's ability to absorb water increases with an increasing swelling rate, thereby increasing the sorption support. The increased hydrophilicity of the catalytic membrane with increasing SSA was supported by interaction parameter values approaching zero. The image of synthesized ZIF-8 crystals obtained by SEM was consistent with the literature. The high crystallinity of ZIF-8 crystals was determined by XRD analysis. The LA conversion obtained in SoLE production with a PVA/SSA functional catalytic membrane at 9 mmol catalyst loading, 105 °C, Solketal/LA molar ratio of 6/1, and a reaction time of 6 hours was 97.65%, while the reaction conversion was 96.81% in SoLE synthesis with a PVA/SSA/ZIF-8 catalytic membrane under the same catalyst loading, temperature, and molar ratio, but with a reaction time of 4 hours. In this reaction, MOF ZIF-8 significantly reduced the reaction time, an improvement that cannot be ignored in terms of system cost. The developed functional catalytic membranes are promising and effective materials for the potential fuel additive SoLE synthesis.

Competing Interests

The authors declare no conflict of interest.

Acknowledgement

This study was supported by the scientific research projects unit of Kocaeli University. Project No: FDK 2023-3201. Additionally, the authors would like to thank Guler Hasirci for her assistance in the preparation of the article.

References

Al-Saadi A., Mathan B., He Y. (2020), Esterification and transesterification over SrO–ZnO/Al₂O₃ as a novel bifunctional catalyst for biodiesel production, *Renewable Energy*, 158, 388–399, dx.doi.org/10.1016/j.renene.2020.05.171

Atkar A., Bajad S. S. G., Deshmukh S., Dinker A., Kishor K. (2024), Synthesis and characterization of sulfonated chitosan (SCS) / sulfonated polyvinyl alcohol (SPVA) blend membrane for microbial fuel cell application, *Materials Science and Engineering B*, 299, 116942, dx. doi.org/10.1016/j.mseb.2023.116942

Attwa M., Said A., ElGamal M., El-Shaer Y., Elbasuney S. (2024),
Bespoke Energetic Zeolite Imidazolate Frameworks-8 (ZIF8)/Ammonium Perchlorate Nanocomposite: A Novel Reactive
Catalyzed High Energy Dense Material with Superior
Decomposition Kinetics, Journal of Inorganic and
Organometallic Polymers and Materials, 34, 387–400,
dx.doi.org/10.1007/s10904-023-02834-2

Çakmak A., Özcan H. (2018), Benzin İçin Oksijenli Yakıt Katkıları, Journal of Polytechnic, 0900, 831–840, dx.doi.org/10.2339/politeknik.457956

Cao M., Peng L., Xie Q., Xing K., Lu M., Ji J. (2021), Sulfonated Sargassum horneri carbon as solid acid catalyst to produce biodiesel via esterification, *Bioresource Technology*, 324, 124614, dx.doi.org/10.1016/j.biortech.2020.124614

Chansorn N., Amnuaypanich S., Soontaranon S., Rugmai S., Amnuaypanich S. (2022), Increasing solketal production from the solventless ketalization of glycerol catalyzed by nanodispersed phosphotungstic acid in poly(N-methyl-4-vinylpyridinium) grafted on silica nanoparticles, *Journal of Industrial and Engineering Chemistry*, 112, 233–243, dx.doi.org/10.1016/j.jiec.2022.05.017

Demirbas A., Balubaid M.A., Basahel A.M., Ahmad W., Sheikh M.H. (2015), Octane Rating of Gasoline and Octane Booster Additives, *Petroleum Science and Technology*, 33, 1190–1197, dx.doi.org/10.1080/10916466.2015.1050506

Doan T. D., Vu N. N., Hoang T. L. G., Nguyen-tri P. (2025), Metalorganic framework (MOF) -based materials for photocatalytic antibacterial applications, *Coord. Chem. Rev.*, 523, 216298, dx.doi.org/10.1016/j.ccr.2024.216298

Ethiraj J., Wagh D., Manyar H. (2022), Advances in Upgrading Biomass to Biofuels and Oxygenated Fuel Additives Using Metal Oxide Catalysts, *Energy and Fuels*, 36, 1189–1204, dx.doi.org/10.1021/acs.energyfuels.1c03346

Fernández P., Fraile J.M., García-Bordejé E., Pires, E. (2019), Sulfonated hydrothermal carbons from cellulose and glucose as catalysts for glycerol ketalization, *Catalysts*, 9, 804, dx.doi.org/10.3390/catal9100804

Goda M.N., Said A.E.A.A., El-Aal M.A. (2022), Mineral acidactivated sugarcane bagasse ash as solid acid catalyst for the liquid phase esterification of acetic acid with n-amyl, benzyl, and n-butyl alcohols, *Journal of Environmental Chemical*

- *Engineering,* 10, 107355, dx.doi.org/10.1016/ j.jece.2022.107355
- Gomaa M.M., Hugenschmidt C., Dickmann M., Abdel-Hamed M.O., Abdel-Hady E.E., Mohamed H.F.M. (2017), Free volume of PVA/SSA proton exchange membrane studied by positron annihilation lifetime spectroscopy, *Acta Physica Polonica A*, 132, 1519–1522, dx.doi.org/10.12693/APhysPolA.132.1519
- Guo M., Jiang W., Chen C., Qu S., Lu J., Yi W., Ding J. (2021), Process optimization of biodiesel production from waste cooking oil by esterification of free fatty acids using La 3 + / ZnO-TiO ₂ photocatalyst, *Energy Conversion and Management*, 229, 113745, dx.doi.org/10.1016/ j.enconman.2020.113745
- Hasirci G., Ilgen O., Hilmioglu N. (2023), Synthesis of the Environmentally Friendly Fuel Bioadditive Solketal by the Green Catalytic Membrane PVA/PAMPS, *Water, Air, & Soil Pollution*, 234, 1–14, dx.doi.org/10.1007/s11270-023-06680-3
- Hilmioglu N. (2022), Optimization of Synthesis of Ethyl Acetate by Response Surface Method and Investigation of Reactive Sorption Effect of Hydrogel in Synthesis, *European Journal of Science and Technology*, 35, 94–101, dx.doi.org/10.31590/ejosat.1061611
- Huang R.Y.M. (1991), Pervaporation Membrane Sepration Processes. Membrane Science and Technology, 1 st edition, New York.
- Ilgen O., Yerlikaya S., Akyurek F.O. (2017), Synthesis of Solketal from Glycerol and Acetone over Amberlyst-46 to Produce an Oxygenated Fuel Additive, *Periodica Polytechnica Chemical Engineering*, 61 (2), 144–148, dx.doi.org/10.3311/PPch.8895
- Jeanmard L., Rongwong W., Chisti Y. (2025), Biomass and Bioenergy Biomass-derived levulinic acid as a platform chemical for making diverse products, *Biomass and Bioenergy*, 195, 107683, dx.doi.org/10.1016/j.biombioe.2025.107683
- Jia S., Ma J., Wang D., Wang K., Zheng Q., Song C., Guo X. (2020), Fast and efficient upgrading of levulinic acid into long-chain alkyl levulinate fuel additives with a tungsten salt catalyst at low temperature, Sustainable Energy & Fuels, 4, 2018–2025, dx.doi.org/10.1039/c9se01287g
- Khatuaa C., Chinyaa I., Sahab D., Dasa S., Sena R., Dhara A. (2015), Modified clad optical fibre coated with PVA/TiO₂ nano composite for humidity sensing application, *International Journal on Smart Sensing and Intelligent Systems*, 8, 1424–1442, dx.doi.org/10.21307/ijssis-2017-813
- Kruk M., Jaroniec M., 2001, Gas Adsorption Characterization of Ordered Organic-Inorganic Nanocomposite Materials, Chemistry of Materials, 13, 10, 3169–3183, dx. doi.org/10.1021/cm0101069
- Laeim H., Molahalli V., Prajongthat P., Pattanaporkratana A., Pathak G., Phettong B., Hongkarnjanakul N., Chattham N. (2025), Porosity Tunable Metal-Organic Framework (MOF) -Based Composites for Energy Storage Applications: Recent Progress, *Polymers*, 17, 130, dx.doi.org/10.3390/ polym17020130
- Li W., Liu W., Xing W., Xu N. (2013), Esterification Of Acetic Acid And N-Propanol With Vapor Permeation Using NaA Zeolite Membrane, *Industrial And Engineering Chemistry Research*, 52, 6336–6342, dx.doi.org/10.1021/ie3031086
- Li Y., Zhu K., Jiang Y., Chen L., Zhang H., Li H., Yang S. (2023), Biomass-derived hydrophobic metal-organic frameworks solid acid for green efficient catalytic esterification of oleic

- acid at low temperatures, *Fuel Processing Technology*, 239, 107558, dx.doi.org/10.1016/j.fuproc.2022.107558
- Liu H., Ma Z., Liu X., Wu Y., Zhang W., Zhao S. (2024), Green synthesis of biobased glycerol levulinate ketal in a continuous flow reactor: Optimization, kinetics and simulation, *Applied Energy*, 361, 122910, dx.doi.org/10.1016/j.apenergy.2024.122910
- Liu Z., Ma Y. (2024), Chemical Recycling of Step-Growth Polymers Guided by Le Chatelier's Principle, *ACS Engineering Au*, 4, 432-449, dx.doi.org/10.1021/acsengineeringau.4c00015
- Liu, J., Shi, J., Zhang, B., Cheng, Z. (2022), Novel Magnetically-Recoverable Solid Acid Catalysts with a Hydrophobic Layer in Protecting the Active Sites from Water Poisoning, *Processes*, 10, 1738, dx.doi.org/10.3390/ pr10091738.
- Maarouf S., Alouane Z., Tazi B., Guenoun F., Fouad K. (2020), Fabrication and properties of hybrid membranes based on poly (vinyl alcohol), sulfosuccinic acid and salts of heteropolyacid with or without silica for fuel cells applications, *Advances in Science, Technology and Engineering Systems*, 5, 1013–1019, dx.doi.org/10.25046/aj0505124
- Mao F.F., Zhao W., Tao D.J., Liu X. (2020), Highly Efficient Conversion of Renewable Levulinic Acid to n-Butyl Levulinate Catalyzed by Sulfonated Magnetic Titanium Dioxide Nanotubes, *Catalysis Letters*, 150, 2709–2715, dx.doi.org/10.1007/s10562-020-03177-0
- Mariam N. N. S., Hoong S.S., Maznee T. N., Arniza M. Z., Yusop R. M. (2024), Solketal Levulinate Ester as a Potential Fuel Additive For Palm Biodiesel, *Journal of Oil Palm Research*, 36, 104–114, dx.doi.org/10.21894/jopr.2023.0004
- Mariam N.N.S., Hoong S.S., Arniza M. Z., Adnan S., Ismail T. N. M. T., Yeong S. K., Yusop M. R. (2021), Optimisation Of Reaction Parameters For The Synthesis Of Solketal Levulinate As Potential Biodiesel Additive, *Journal of Oil Palm Research*, 34(3), 524-534, dx.doi.org/10.21894/jopr.2021.0052
- Milne A. J. B. and Amirfazli A. (2009), Drop Shedding by Shear Flow for Hydrophilic to Superhydrophobic Surfaces, *Langmuir*, 25(24), 14155–14164, dx.doi.org/10.1021/la901737y.
- Missaoui N., Kahri H., Demirci U. B., 2022, "Rapid room-temperature synthesis and characterizations of high-surface-area nanoparticles of zeolitic imidazolate framework-8 (ZIF-8) for CO2 and CH4 adsorption", Journal of Materials Science, 57, 16245–16257, dx. doi.org/10.1007/s10853-022-07676-w
- Moradi P., Saidi M., Najafabadi A.T. (2021), Biodiesel production via esterification of oleic acid as a representative of free fatty acid using electrolysis technique as a novel approach: Noncatalytic and catalytic conversion, *Process Safety and Environmental Protection*, 147, 684–692, dx.doi.org/10.1016/j.psep.2020.12.032
- Mussatto S.I., Dragone G., Guimarães P.M.R., Silva J.P.A., Carneiro
 L.M., Roberto I.C., Vicente A., Domingues L., Teixeira J.A.
 (2010), Technological trends, global market, and challenges of bio-ethanol production, *Biotechnology Advances*, 28, 817–830, dx.doi.org/10.1016/j.biotechadv.2010.07.001
- Ngo H.L., Nguyen N.T., Ho T.T.N., Pham H.V., Le T.N., Tran T.N., Huynh L.T.N., Pham T.N., Nguyen T.T., Nguyen T.H., Le V.H., Tran D.L. (2022), The performance of MCDI: the effect of sulfosuccinic acid ratio in the PVA-based cation exchange membrane, *lonics*, 28, 4369–4380, dx.doi.org/10.1007/s11581-022-04661-w

Nistane J., Chen L., Lee Y., Lively R., Ramprasad R. (2022), Estimation of the Flory-Huggins interaction parameter of polymer-solvent mixtures using machine learning, *MRS Communications*, 12, 1096–1102, dx.doi.org/10.1557/s43579-022-00237-x

- Nordin N. A. H. M., Ismail A. F., Yahya N. (2017), Zeolitic imidazole framework 8 decorated graphene oxide (ZIF-8/GO) mixed matrix membrane (MMM) for CO₂/CH₄ separation, *Jurnal Teknologi-Sciences & Engineering*, 79, 59–63, doi.org/10.11113/jt.v79.10438
- Norouzi M.A., Montazer M., Harifi T., Karimi P. (2021), Flower buds like PVA/ZnO composite nanofibers assembly: Antibacterial, in vivo wound healing, cytotoxicity and histological studies, *Polymer Testing*, 93, 106914, dx.doi.org/10.1016/j.polymertesting.2020.106914
- Ohtake T., Ito H., Horiba K., Toyoda N. (2022), Synthesis of Water-Soluble Polymeric Surfactants Bearing Sulfonic Acid Groups and the Effects of Hydrophilic Components on the Rheology and Dispersive Properties of Dye Dispersions, *ACS Applied Polymer Materials*, 4, 8556–8563, dx.doi.org/10.1021/acsapm.2c01471
- Pan Y., Liu Y., Zeng G., Zhao L., Lai Z. (2011), Rapid synthesis of zeolitic imidazolate framework-8 (ZIF-8) nanocrystals in an aqueous system, *Chemical Communications*, 47, 2071–2073, dx.doi.org/10.1039/C0CC05002D
- Pan Y., Liu Y., Zeng G., Zhaoa L., Lai Z., 2011, Rapid synthesis of zeolitic imidazolate framework-8 (ZIF-8) nanocrystals in an aqueous system, Chemical Communication, 47, 2071-2073, dx. doi.org/10.1039/C0CC05002D
- Portillo Perez G. A., Pandey S., Dupont M. J. (2023), Sulfosuccinic acid-based metal-center catalysts for the synthesis of HMF from carbohydrates, *Catalysis Today*, 418, 1–11, dx.doi.org/10.1016/j.cattod.2023.114127
- Qiu K., Shu Y., Zhang J., Gao L., Xiao G. (2022), Effective and Stable Zeolite Imidazole Framework-Supported Copper Nanoparticles (Cu/ZIF-8) for Glycerol to Lactic Acid, *Catalysis Letters*, 152, 172–186, dx.doi.org/10.1007/s10562-021-03610-y
- Rezaee R., Nasseri S., Mahvi A. H., Nabizadeh R., Mousavi S. A., Rashidi A., Jafari A., Nazmara S. (2015), Fabrication and characterization of a polysulfone-graphene oxide nanocomposite membrane for arsenate rejection from water, *Journal of Environmental Health Science and Engineering*, 213(61), dx.doi.org/10.1186/s40201-015-0217-8
- Ristiana D. D., Suyanta S., Nuryono N. (2022), Sulfonic acid-functionalized silica with controlled hydrophobicity as an effective catalyst for esterification of levulinic acid, *Materials Today Communications*, 32, 103953, dx.doi.org/10.1016/j.mtcomm.2022.103953.
- Rynkowska E., Fatyeyeva K., Kujawa J. (2019), Chemically and Thermally Crosslinked PVA-Based Membranes: Effect on Swelling and Transport Behavior, *Polymers*, 11, 1799, dx.doi.org/10.3390/polym11111799
- Sajid M., Farooq U., Bary G., Azim M. M., Zhao X. (2021), Sustainable production of levulinic acid and its derivatives for fuel additives and chemicals: progress, challenges, and prospects, *Green Chemistry*, 23, 9198–9238, dx.doi.org/10.1039/d1gc02919c
- Sann E. E., Pan Y., Gao Z., Zhan S., Xia F. (2018), Highly hydrophobic ZIF-8 particles and application for oil-water separation, Separation and Purification Technology, 206, 186–191, dx.doi.org/10.1016/j.seppur.2018.04.027

Sann E. E., Pan Y., Gao Z., Zhan S., Xia F. (2018), Highly hydrophobic ZIF-8 particles and application for oil-water separation, Separation and Purification Technology, 206, 186–191.

- Singh P.K., Kumar S.S., Lakshmana Kumar S., Kulandaivel A., Geerthik S., Ganeshan P., Sathish Kannan, S., Seikh, A.H., Iqbal A. (2023), Impact of oxy-additives on diesel engine performance and emission parameters using waste cooking oil biodiesel, *Global NEST Journal*, 25, 105–112, dx.doi.org/10.30955/gnj.004983
- Soltani S., Khanian N., Shean T., Choong Y., Asim N., Zhao Y. (2021), Microwave-assisted hydrothermal synthesis of sulfonated TiO 2 -GO core – shell solid spheres as heterogeneous esterification mesoporous catalyst for biodiesel production, *Energy Conversion and Management*, 238, 114165, dx.doi.org/10.1016/j.enconman.2021.114165
- Song W., Zhao X., Jin Z., Fan L., Ji, X. (2023), Poly (vinyl alcohol) for multi-functionalized corrosion protection of metals: A review, *Journal of Cleaner Production*, 394, 136390, dx.doi.org/10.1016/j.jclepro.2023.136390
- Suryandari A. S., Nurtono T., Widiyastuti W., Setyawan H. (2023), Hydrophobic Modification of Sulfonated Carbon Aerogels from Coir Fibers To Enhance Their Catalytic Performance for Esterification, *ACS Omega*, 8, 27139–27145, dx.doi.org/10.1021/acsomega.3c02244.
- Sutinno, S. (2016), Esterification of Solketal And Levulinic Acid Over Heterogeneous Acid Catalysts, Degree of Master Thesis, Petrochemistry and Polymer Science, Chulalongkorn University.
- Thanh M. T., Thien T. V., Chau V.T. T., Du P. D., Hung N. P., Khieu D. Q. (2017), Synthesis of Iron Doped Zeolite Imidazolate Framework-8 and Its Remazol Deep Black RGB Dye Adsorption Ability, *Journal of Chemistry*, 2017, 1-18, dx.doi.org/10.1155/2017/5045973
- Unlu D., Hilmioglu N. D. (2016), Environmental Effects Fuel bioadditive production by chitosan / sulfosuccinic acid catalytic membrane, *Energy Sources, Part A: Recovery, Utilization, and Environmental Effects*, 38, 3606–3611, dx.doi.org/10.1080/15567036.2016.1166166
- Unlu D., Hilmioglu N. D. (2019), Production of Fuel Bioadditive "Triacetin" Using a Phosphomolybdic-Acid-Loaded PVA Membrane in a Pervaporation Catalytic Membrane Reactor, Energy Fuels, 33, 2208-2218, dx.doi.org/10.1021/acs.energyfuels.8b03344
- Wi'sniewska P., Haponiuk J., Saeb M, R., Rabiee N., Bencherif S. A. (2023), Mitigating metal-organic framework (MOF) toxicity for biomedical applications, *Chemical Engineering Journal*, 471, 144400, dx.doi.org/10.1016/j.cej.2023.144400
- Xu Y., Guo P., Chang C., Li P., Zhao S., Xu G. (2020), Aluminum chloride-catalyzed conversion of levulinic acid to methyl levulinate: optimization and kinetics, *Journal of Chemical Technology & Biotechnology*, 95, 2251–2260, dx.doi.org/10.1002/jctb.6413
- Yadav D., Karunanithi A., Saxena S., Shukla S. (2022), Modified PVA membrane for separation of micro-emulsion, *Science of the Total Environment*, 822, 153610, dx.doi.org/10.1016/j.scitotenv.2022.153610
- Yagizatli Y., Sahin A., Ar I. (2022), Effect of thermal crosslinking process on membrane structure and PEM fuel cell applications performed with SPEEK-PVA blend membranes, *International Journal of Hydrogen Energy*, 47, 40445–40461, dx.doi.org/10.1016/j.ijhydene.2022.04.183

- Yang F., Wu J., Zhu X., Ge T., Wang R. (2021), Enhanced stability and hydrophobicity of LiX@ZIF-8 composite synthesized environmental friendly for CO₂ capture in highly humid flue gas, *Chemistry Engineering Journal*, 410, 128322, dx.doi.org/10.1016/j.cej.2020.128322
- Zhang B., Gao M., Geng J., Cheng Y., Wang X., Wu C., Wang Q., Liu S., Cheung S.M. (2021), Catalytic performance and deactivation mechanism of a one-step sulfonated carbon-based solid-acid catalyst in an esterification reaction, Renewable Energy, 164, 824–832, dx.doi.org/10.1016/j.renene.2020.09.076
- Zhang K., Lively R. P., Zhang C., Chance R. R., Koros W. J., Sholl D. S., Nair S. (2013), Exploring the Framework Hydrophobicity and Flexibility of ZIF-8: From Biofuel Recovery to Hydrocarbon Separations, *The Journal of Physical Chemistry Letters*, 4, 3618–3622, dx.doi.org/10.1021/jz402019d.
- Zhang M., Ming J., Zhang W., Xie J., Lin P., Song X., Chen X., Wang X., Zhou B., 2022, Porous Organic Polymer-Derived

- Fe2P@N,P-Codoped Porous Carbon as Efficient Electrocatalysts for pH Universal ORR, ACS Omega, 5, 7225–7234, dx. doi.org/10.1021/acsomega.2c00216
- Zhang Q., Hong X., Lei J., Lei Y., Yang Y., Cheng J., Hu Y., Zhang Y. (2024), Environmentally-friendly preparation of Sn(II)-BDC supported heteropolyacid as a stable and highly efficient catalyst for esterification reaction, *Journal of Saudi Chemical Society*, 28, 101832, dx.doi.org/10.1016/j.jscs.2024.101832
- Zhu Jie., Li L., Cao M. (2024), Le Chatelier's principle to stabilize intrinsic surface structure of oxygen-evolving catalyst for enabling ultra-high catalytic stability of zinc-air battery and water splitting, *Nano Energy*, 122, 109300, dx.doi.org/10.1016/j.nanoen.2024.109300
- Zhu Jishen., Jiang W., Yuan Z., Lu J., Ding J. (2024), Taguchi method for optimizing the cation exchange resin catalyzed esterification of oleic acid with ethanol and adsorption kinetics study, *Process Safety and Environmental Protection*, 182, 989–998, dx.doi.org/10.1016/j.psep.2023.12.052